

1 **Littoral steering of deltaic channels**

2 Jaap Nienhuis^{1,2*}, Andrew D. Ashton¹, Liviu Giosan¹

3 ¹Department of Geology and Geophysics, Woods Hole Oceanographic Institution, Woods Hole,
4 MA

5 ²Earth, Atmospheric and Planetary Sciences, Massachusetts Institute of Technology, Cambridge,
6 MA

7 * Corresponding author current address: Department of Earth and Environmental Sciences,
8 Tulane University, New Orleans, LA, jnienhui@tulane.edu

9 **Abstract**

10 The typically single-threaded channels on wave-influenced deltas show striking
11 differences in their orientations, with some channels oriented into the incoming waves (e.g.,
12 Ombrone, Krishna), and others oriented away from the waves (e.g., Godavari, Sao Francisco).
13 Understanding the controls on channel orientation is important as the channel location greatly
14 influences deltaic morphology and sedimentology, both subaerially and subaqueously. Here, we
15 explore channel orientation and consequent feedbacks with local shoreline dynamics using a
16 plan-form numerical model of delta evolution. The model treats fluvial sediment delivery to a
17 wave-dominated coast in two ways: 1) channels are assumed to prograde in a direction
18 perpendicular to the local shoreline orientation and 2) a controlled fraction of littoral sediment
19 transport can bypass the river mouth. Model results suggest that channels migrate downdrift
20 when there is a significant net littoral transport and alongshore transport bypassing of the river
21 mouth is limited. In contrast, river channels tend to orient themselves into the waves when
22 fluvial sediment flux is relatively large, causing the shoreline of the downdrift delta flank to
23 attain the orientation of maximum potential sediment transport for the incoming wave climate.
24 Using model results, we develop a framework to estimate channel orientations for wave-
25 influenced deltas that shows good agreement with natural examples. An increase in fluvial
26 sediment input can cause a channel to reorient itself into incoming waves, behavior observed, for
27 example, in the Ombrone delta in Italy. Our results can inform paleoclimate studies by linking
28 channel orientation to fluvial sediment flux and wave energy. In particular, our approach
29 provides a means to quantify past wave directions, which are notoriously difficult to constrain.

30 **1 Introduction**

31 Major channels of wave-influenced deltas tend to be straight, or gently curving, rather
32 than meandering, with orientations that can diverge from the upland river course. It has been
33 hypothesized that a delta's channel orientation arises from the interaction between fluvial
34 channel-building processes and littoral sediment transport at the shoreline (Bhattacharya and
35 Giosan, 2003; Pranzini, 2001). However, the controls on channel orientation are not
36 straightforward as, on some deltas, channels turn into the waves, whereas, on other deltas,
37 channels migrate away from the waves (Fig. 1). The presence of the channel itself affects coastal
38 processes, as river mouths can limit bypassing of littoral sediment (Nienhuis et al., 2016). As
39 such, a mechanistic understanding of the basic controls on channel orientation has been
40 previously lacking. To investigate the mechanisms and controls that set the channel orientations
41 on wave-influenced deltas, we have conducted experiments using an exploratory model of plan-
42 view delta evolution. In these experiments, we allow local shoreline dynamics to determine the
43 channel orientation, while also controlling the quantity of littoral sediment that can bypass the
44 river channel. We compare these model experiments to natural examples in a mechanistic
45 framework, which not only allows us to predict the channel orientation for modern deltas, but
46 also, as the channel orientation of wave-influenced deltas is preserved in the morphology of
47 deltas and eventually stored in the stratigraphic record, has the potential to inform us about past
48 and present fluvial and alongshore sediment transport fluxes.

49 2 Background

50 2.1 *Asymmetric Wave-influenced Deltas*

51 In the absence of waves, river deltas often develop intricate networks of distributary
52 channels resulting from mouth-bar formation and channel avulsions (Geleynse et al., 2011;
53 Wright, 1977). However, waves inhibit mouth bar formation and move sediment alongshore, and
54 as such can suppress the emergence of small-scale distributaries, generally leading to the growth
55 of a single major channel (Wright and Coleman, 1973) and a cusped delta shape (Grijm, 1960).

56 Alongshore transport of fluvial sediment is the primary mechanism shaping wave-
57 influenced deltas (Bakker and Edelman, 1964; Tanner, 1958). Waves breaking at an angle to the
58 coastline drive a flux of sediment alongshore (Komar, 1971); this flux is maximized for
59 incoming waves with an offshore direction of about 45 degrees (Fig. 2, see also Ashton and
60 Murray, 2006a, 2006b). Alongshore sediment transport also defines when a delta adopts a
61 cusped, wave-dominated morphology. If the fluvial sediment supply is less than the maximum
62 potential alongshore sediment transport (the maxima in Fig. 2a), both flanks of a delta can be
63 oriented such that the fluvial supply of coarse-grained shore-compatible sediment is transported
64 away from the river mouth by alongshore sediment transport (Nienhuis et al., 2015).

65 Because of the angle dependence of alongshore sediment transport (Fig. 2a), oblique
66 waves can generate a net alongshore drift that can result in delta plan-view asymmetry,
67 particularly if fluvial sediment input is relatively large (Ashton and Giosan, 2011; Bhattacharya
68 and Giosan, 2003). In asymmetric deltas, accumulating sediments come not only from the “dip-

69 feeding” river but also from updrift sources via the wave-driven “strike-feeding” littoral region
70 (Ashton and Giosan, 2011; Dominguez, 1996; Giosan, 1998).

71 To characterize the morphologic and sedimentological asymmetry of deltas, Bhattacharya
72 and Giosan (2003) proposed an asymmetry index, A: net alongshore sediment transport at the
73 river mouth (in m^3yr^{-1}) divided by river water discharge (in $10^6 \text{ m}^3\text{month}^{-1}$). For low values of A
74 (<200), deltas tend to be symmetric, and both delta flanks have similar morphologies. For large
75 values of A (>200), deltas are asymmetric and the updrift flank is sourced from the littoral
76 system whereas the downdrift flank is composed of fluvial sediments. For example, in its later
77 history the Sao Francisco delta built beach plains on its north (updrift) side, whereas fluvial fine-
78 grained sediments fed the downdrift and accumulated, interspersed with beach ridges, on the
79 south side flank (Fig. 1b, Dominguez, 1996). Depending on the balance between fluvial and
80 marine controls, delta or delta lobe asymmetry can change during growth (Bhattacharya and
81 Giosan, 2003; cf., Rossetti et al., 2015). A quantitative framework of deltaic channel orientation
82 has therefore the potential to strengthen interpretations of the sedimentary architecture of deltas.

83 2.2 *Channels on Deltas*

84 Deltaic distributary channels are generally devoid of meanders that are common on
85 many alluvial channels farther upstream (Jerolmack and Mohrig, 2007). The absence of
86 meanders is a direct result of the lack of lateral channel migration (Hudson and Kesel, 2000;
87 Kolb, 1963). Lamb et al. (2012) postulated that backwater dynamics create an efficient fluvial
88 sediment transport regime through the lower reaches of a deltaic channel, limiting point bar
89 formation and meander initiation on the delta plain. In the absence of post-depositional lateral

90 migration mechanisms, deltaic channel patterns must therefore be the result of depositional
91 history at the delta coastline (e.g., Bates, 1953).

92 However, controls on the channel orientation of wave-influenced deltas are not
93 straightforward; channels can be directed either along with or against the direction of net littoral
94 drift. For example, the Ombrone delta (Fig. 1a) is oriented into the direction of wave approach.
95 Other deltaic channels (e.g. Nile, Sao Francisco) have migrated away from the waves (Fig. 1b,
96 1c), or display no dominant direction (Fig. 1d).

97 Investigating the orientation of small streams along the coast, Gulliver (1896) noted that
98 stream deflections follow nearshore currents, which Zenkovich (1967) attributed to breaking-
99 wave-driven alongshore sediment transport. Pranzini (2001) demonstrated how the channels of
100 the Ombrone and the Arno delta have changed their orientation over time, suggesting that the
101 channels rotated into the direction of net alongshore drift during a period of increased sediment
102 load associated with land use changes. He noted that delta progradation into a more pointy
103 cusped shape increased the wave energy per meter of coast on the updrift flank but decreased
104 wave energy on the downdrift flank. In this model, wave energy imbalance can increase
105 sediment transport away from the river mouth along the updrift flank, reorienting the channel
106 into the direction of wave approach (Pranzini, 2001).

107 Although the coupling between alongshore sediment transport and channel orientation
108 appears to be intuitive, there have been no studies to date that offer a predictive characterization
109 of channel orientation, or studies that have shown how the continuum of delta morphologies
110 could lead to a continuum of channel orientations.

111 2.3 *Alongshore Sediment Bypassing the River Mouth*

112 A river mouth can act as a ‘hydraulic groin’ along a sandy coastline and partially or
113 entirely block alongshore transport, trapping sediments updrift and limiting supply to downdrift
114 beaches (Zenkovich, 1967). Littoral sediment that is blocked by the river mouth can form river
115 mouth spits and initiate river mouth migration (Dominguez, 1996; Zenkovich, 1967). Aibulatov
116 and Shadrin (1961) used tracers to study littoral sediment bypassing the river mouth and found
117 transport pathways around the river mouth bar. Another study, by Balouin et al. (2006), found
118 that sediment can also be bypassed through the channel to the downdrift beach. Investigating
119 controls on bypassing, Kirk (1991) observed that river mouths tend to low bypassing rates at
120 moderate discharge conditions and high bypassing rates for low discharge conditions. This
121 tendency for increased discharge to lead to decreased bypassing has also been demonstrated
122 using numerical modeling experiments (Nienhuis et al., 2016). A dependence on discharge
123 would give alongshore sediment bypassing a strongly seasonal character (Cooper, 1994).

124 Sediment bypassing occurs on longer timescales at distributary mouths of large wave-
125 dominated deltas (Bhattacharya and Giosan, 2003). Subaqueous shoals that develop during
126 floods can lead to a feedback between the trapping of fluvial sediment near the river mouth and
127 the blocking and redistribution of littoral sediments that further expands the subaqueous delta
128 (Giosan et al., 2005). Eventual emergence, elongation, and amalgamation of river mouth islands
129 transforming into spits that then attach to the delta coast represents a long-term bypassing
130 mechanism with timescales of multiple centuries. On the Danube delta, bypassing is intertwined
131 with the simultaneous dynamics of littoral transport along the wave-dominated coastline (Giosan,
132 2007; Giosan et al., 2013). Bypassing and other river mouth processes could affect the delta

133 channel orientation by controlling the partitioning of fluvial and littoral sediments between both
134 delta flanks.

135 2.4 *Modeling Wave-influenced Deltas*

136 The plan-view dynamics of wave-influenced deltas has been modeled analytically
137 (Bakker and Edelman, 1964; Grijm, 1960; Larson et al., 1987) and numerically (Ashton and
138 Giosan, 2011; Komar, 1973; Nienhuis et al., 2013). These previous models have assumed a fixed
139 channel orientation, typically perpendicular to the regional shoreline trend with sediment
140 deposition modeled as a point source at the river mouth. In the model of Larson et al. (1987),
141 alongshore sediment transport is linearly related to the wave approach angle (small angle
142 approximation of the CERC equation, Fig. 2a), which reduces coastal evolution to a classic
143 diffusion problem with no morphologic differences between the updrift and downdrift delta
144 flank. Accounting for non-linearity but not for wave refraction, Bakker and Edelman (1964)
145 demonstrate how oblique wave incidence can result in a morphologic groin effect: preferential
146 growth of the updrift delta flank when shoreline instability, and an associated decrease in
147 alongshore sediment transport, occurs along the downdrift flank.

148 More recently, Ashton and Giosan (2011) studied the effect of a distribution of wave
149 angles on wave-influenced deltas in the Coastline Evolution Model (CEM, Ashton and Murray,
150 2006a). The model results, which account for non-linearity and wave refraction, suggest that the
151 morphologic groin effect occurs due to a decrease in wave height along the downdrift coast, even
152 when waves break at relatively small angles. Furthermore, Ashton and Giosan (2011) suggest
153 that the spread of incoming wave directions acts as an important control on the delta plan-view

154 shape and progradation rate. Further analytical exploration by Nienhuis et al. (2015) suggest that
155 the distribution of incoming waves can even control whether a delta will attain a wave-
156 dominated or river-dominated morphology. Using CEM, Ashton et al. (2013) modeled two
157 channels that randomly rotate laterally. By coupling channel length via channel slope to the
158 fluvial sediment flux partitioning, their study showed that feedbacks tend to equilibrate channel
159 lengths and result in more regularly cusped delta shapes even with multiple active distributaries.
160 All of these previous model applications treated the river mouth solely as an additional sediment
161 source—littoral sediment was freely able to bypass the river mouth.

162 Here, we expand upon previous studies by incorporating two aspects of wave-dominated
163 deltas that have not yet been accounted for: (1) the potential for feedbacks at the shoreline to
164 reorient the channel course, and (2) the ability of the river mouth to block bypassing of some of
165 the alongshore sediment transport flux. We use an exploratory modeling approach (Murray,
166 2003) to analyze and quantify the potential effect of wave climate, fluvial sediment load, and
167 alongshore sediment bypassing on channel orientation.

168 **3 Methods**

169 *3.1 Coastline Evolution Model*

170 To investigate the controls on channel orientation, we modified the existing plan-view
171 model of shoreline dynamics CEM (see Ashton and Murray, 2006a). CEM assumes a constant
172 shoreface cross-sectional profile such that the divergence of littoral fluxes along the coast
173 corresponds directly to advance or retreat of the shoreline position (Ashton and Murray, 2006a;
174 Ashton et al., 2001). Assuming refraction over shore-parallel shoreface contours, the wave

175 energy and wave direction then drive a sediment flux alongshore (Q_s), calculated with the CERC
176 formula for littoral transport (Fig. 2a, Komar, 1971). The plan-view domain is divided into cells
177 (cell size is 40 m) that are filled (land), empty (sea) or partially filled (shoreline). The percentage
178 filled in each cell sets the cross-shore location of the shoreline within the cell and is used to
179 calculate the shoreline orientation with respect to neighboring cells (Fig. 3a, Ashton and Murray,
180 2006a).

181 Every time step (one day), the model picks a deep-water wave direction from a
182 probability distribution function representing the directional wave climate. We define the
183 directional spectrum of incoming waves using two parameters: the fraction of waves coming
184 from the left looking offshore (wave asymmetry, A), and the fraction of waves coming
185 approaching from high angles ($|\phi-\theta| > 45$, H , see Fig. 2b). In our model experiments, we have
186 varied the wave asymmetry A between 0.5 and 0.8, the high-angle proportion H between 0.1 and
187 0.3, and the wave height between 0.8 and 1.2 meters. We use a constant wave period of 5
188 seconds.

189 3.2 *Fluvial Sediment Flux and Dynamic Channel Orientation*

190 To represent a fluvial sediment source in the CEM, one cell along the shoreline is defined
191 as the river mouth cell (using a method described below) and includes a fluvial sediment flux
192 (Q_r) in addition to the littoral sediment flux. We assume that fine-grained fluvial sediment is
193 transported offshore by wave suspension and that the coarse-grained sediment directly
194 amalgamates to the shoreface (Ashton and Giosan, 2011). The fluvial sediment flux (Q_r) should
195 therefore be interpreted as the coarse-grained or sand load fraction of the total fluvial sediment

196 flux. By using periodic boundary conditions, the model assumes that deltas grow out along an
197 infinitely long sandy coastline with a continuous supply of sediment from the updrift delta coast.

198 Ashton and Giosan (2011) and Ashton et al. (2013) modified the CEM such that straight
199 channels grew from a nodal point upstream on the delta plain, either in a predefined or randomly
200 selected direction. Channel direction was therefore independent of local shoreline conditions.
201 Here, we have modified CEM such that the channel no longer grows in a predefined direction,
202 instead allowing feedbacks between the shoreline and fluvial sediment delivery to the coast to
203 redirect the channel. To allow these feedbacks, we apply a phenomenological rule, a type of
204 ansatz, such that the river grows perpendicularly to the local shoreline orientation set by the
205 channel's two neighboring cells (Fig 3b).

206 This shore-perpendicular approach is the adoption of the idea that river mouth
207 morphology acts as the primary control on river mouth hydrodynamics and the resulting
208 sedimentation and erosion patterns (Roelvink et al., 1998): if sediment is primarily deposited on
209 one end of the channel, this would likely redirect the flow such that the resulting deposition
210 would become more perpendicular to the local topography contours. Although there is an *ad hoc*
211 element to this river steering rule, analysis of several deltas worldwide shows that the channel
212 trajectory is often perpendicular to the local (~100 m) shoreline orientation, typically varying by
213 only a few degrees (Supplemental Materials Table 1). Our model results therefore act in part as a
214 test of this shore-perpendicular growth rule, which, in keeping with our exploratory modeling
215 approach, allows us to examine feedbacks between shoreline orientation and channel direction.

216 Sensitivity tests show that the channel path is not sensitive to grid resolutions between 20 m and
217 100 m.

218 3.3 *Channel Bypassing*

219 The other modification to CEM is a limit to the amount of littoral sediment flux that is
220 allowed to bypass the river mouth. If there is a sediment flux from a neighboring cell into the
221 river mouth cell, only a fraction of this alongshore sediment flux, β (the bypassing fraction), is
222 allowed to move into the river mouth cell (Fig. 3b). When $\beta = 0$, the river mouth acts as a perfect
223 groin and blocks all the updrift sediment. For $\beta = 1$, as in the original model of Ashton and
224 Giosan (2011), all sediment is freely able to bypass the river mouth, and sediment transport
225 across the river mouth is only based on the local shoreline orientation. The bypassing fraction
226 applies to each wave condition, and therefore the river can block sediment transport across the
227 mouth cell from both the left and right neighbors.

228 Note that we do not model river mouth processes directly, rather we assume an average
229 sediment bypassing fraction and investigate its effects on delta dynamics. Even though the
230 assumption of a constant bypassing fraction is a simplification of the natural bypassing process,
231 our approach allows for straightforward understanding of the end member cases $\beta = 0$ and $\beta = 1$,
232 and is in keeping with our exploratory modeling approach. We ran model experiments for fluvial
233 sediment fluxes between 10 kgs^{-1} and 80 kgs^{-1} and for β of 0, 0.5, and 1.

234 4 Results

235 4.1 Styles of Channel Orientation

236 We have modeled delta formation under different scenarios by varying fluvial sediment
237 supply (Q_r), wave energy, angular wave distribution, and alongshore sediment bypassing (β) to
238 investigate morphologic control on deltaic channel orientation. After ~ 10 model years under
239 constant forcing (Q_r , β , and wave climate), modeled deltas reach a dynamic steady state at the
240 river mouth, with intermittent variability in river channel orientation arising from the stochastic
241 wave angle selection. At this steady state, deltas continue to grow with constant (or near
242 constant) shoreline orientation and channel orientation (Fig. 4).

243 We observe three styles of delta growth based upon channel orientation: (i) *symmetric*
244 *growth*, (ii) *downdrift migration*, and (iii) *updrift migration* (Fig. 4). As expected, symmetrical
245 wave climates build symmetric deltas because there is no net alongshore sediment flux across the
246 river mouth and the shoreline angles on both flanks remain identical. However, symmetric
247 growth also occurs for asymmetrical wave climates for low Q_r and full bypassing (Fig. 4). In this
248 case, shoreline reorientation is limited such that the small angle approximation of the alongshore
249 sediment transport function is appropriate; alongshore transport remains linearly related to the
250 shoreline angle (Fig. 2a) and the shoreline orientations close to the river mouth remain
251 symmetric. If river mouth bypassing is limited and Q_r is low, the channel migrates downdrift.
252 However, for higher Q_r , channels migrate updrift into the direction of dominant wave approach,
253 an effect that is accentuated by low alongshore sediment bypassing (Fig. 4).

254 4.2 Framework for Analyzing Wave-influenced Deltas

255 To understand the controls on channel orientation, we next sought to identify the
256 sediment transport fluxes driving morphologic change. Three key sediment fluxes affect the
257 morphology of the modeled wave-influenced deltas. Q_r is the fluvial sediment flux that is
258 retained nearshore and therefore contributes to the cusate shape of the delta. $Q_{s,regional}$ is the
259 regional, “strike-feeding” (Dominguez, 1996) net alongshore sediment flux (kgs^{-1}). This regional
260 flux is driven by asymmetry in the wave climate and is therefore independent of the river’s
261 influence on the delta shoreline. The alongshore sediment transport tends towards $Q_{s,regional}$ far
262 away from both the left and right delta flanks (Fig. 5a, d). The third important sediment flux, set
263 by the wave climate, is the maximum potential gross alongshore sediment flux $Q_{s,max}$, the sum of
264 the maxima in sediment transport on the updrift, $Q_{s,u,max}$, and downdrift, $Q_{s,d,max}$, flanks for a
265 given wave climate. Along each flank, the maximum potential flux occurs when waves approach
266 the shoreline at approximately 45° (Fig. 2a), but can occur at other orientations for a distribution
267 of wave approach angles (Nienhuis et al., 2015).

268 For a set of environmental conditions (model inputs or for a natural delta setting), these
269 three fluxes Q_r , $Q_{s,regional}$, and $Q_{s,max}$ can be known *a priori* and can therefore be used in a
270 predictive framework to understand consequent delta dynamics. Following Nienhuis et al.
271 (2015), we define the *River Dominance Ratio*:

$$R = \frac{Q_r}{Q_{s,max}}, \quad (1)$$

272 which measures how wave-influenced a river delta is. If $R > 1$, fluvial sediment supply (Q_r) is
273 larger than what waves can maximally transport away along the left and right delta flank, which
274 should tend towards a river-dominated delta morphology.

275 We also define a second non-dimensional number comparing the regional alongshore
276 sediment flux (driven by the wave climate asymmetry) to the fluvial sediment flux. The *Sediment*
277 *Source Ratio*:

$$S = \frac{Q_{s,regional}}{Q_r}, \quad (2)$$

278 defines the relative littoral flux asymmetry of a delta. For $S = 0$, the wave climate is symmetrical
279 and there is no net regional alongshore sediment transport. For $S > 1$, the long term, net
280 alongshore transport of sediment to the delta from the updrift coastline exceeds the fluvial
281 sediment supply, independent of river mouth dynamics.

282 4.3 Littoral Transport along Wave-influenced Deltas

283 Because our modeled deltas reach a dynamic equilibrium configuration, associated
284 alongshore sediment transport fluxes correspondingly reach a long-term steady state that can
285 help explain the mechanisms controlling channel orientation. We calculate the net littoral flux by
286 summing the alongshore sediment transport contributions for a given shoreline orientation across
287 the entire wave climate, taking into account shadowing of waves by other portions of the coast
288 (Fig. 3a).

289 Approaching the river mouth from updrift (the left side for our model experiments), the
290 alongshore sediment transport decreases, and can even reverse direction (Fig. 5d). Alongshore
291 sediment transport increases linearly near the river mouth—a constant divergence of flux
292 corresponds to a constant shoreline accretion rate, demonstrating that the modeled deltas are
293 growing at a steady state.

294 At the river mouth, the delta shoreline abruptly reorients to accommodate the fluvial
295 sediment flux, Q_r (Fig. 5d). We define $Q_{s,u}$ and $Q_{s,d}$ as the alongshore sediment transport
296 immediately updrift and downdrift of the river mouth, respectively, and the maximum potential
297 alongshore sediment transport along the flanks as $Q_{s,u} = Q_{s,u,max}$ and $Q_{s,d} = Q_{s,d,max}$. Note that if
298 sediment is transported along the updrift flank towards the river mouth, $Q_{s,u}$ is positive, whereas
299 a negative $Q_{s,u}$ indicates a reversal in the transport direction driven by delta growth.

300 4.4 Controls on channel orientation

301 We now apply this framework based upon alongshore and fluvial fluxes to better
302 understand the mechanisms behind the observed model behaviors. This allows us to develop
303 quantitative metrics that can predict the degree of downdrift or updrift migration depending on
304 quantities determined by the delta environment: the offshore wave climate ($Q_{s,regional}$, $Q_{s,max}$), the
305 fluvial sediment flux (Q_r), and the fraction of river mouth bypassing (β). As these quantities are
306 exogenous, we can then apply our framework to both modeled and natural examples.

307 4.4.1 Symmetric Growth

308 For small symmetric deltas with non-migrating channels, shoreline reorientation is
309 symmetrical on both flanks, leading to $Q_{s,u} = Q_{s,regional} - \frac{1}{2} Q_r$, and $Q_{s,d} = Q_{s,regional} + \frac{1}{2} Q_r$ (Fig.

310 5d, Case A). The reorientation of the coastline remains symmetric (or nearly so) as long as
311 alongshore sediment transport along the downdrift flank of the delta ($Q_{s,d}$) is less than the
312 maximum potential alongshore sediment transport along the downdrift flank ($Q_{s,d,max}$) (Fig. 5e,
313 Case A).

314 4.4.2 Downdrift Migration

315 Downdrift migration occurs when river mouth bypassing is limited ($\beta < 1$) (Fig. 6) and
316 fluvial sediment supply is low such that alongshore sediment transport on the updrift flank is
317 oriented towards the river mouth ($Q_{s,u} > 0$, Fig. 5d). When downdrift migration occurs, the
318 downdrift shoreline is oriented at a higher angle than the updrift shoreline, typically at or close to
319 the angle of maximum transport (indicated by the magnitude of the transport flux, Fig. 5e).
320 Interestingly, bypassing does not appear to affect the shoreline angle updrift of the river mouth:
321 $Q_{s,u}$ is the same for no bypassing and bypassing scenarios at identical Q_r (Fig. 5e).

322 To formulate an *a priori*, necessary condition for downdrift migration, we cast $Q_{s,u}$ into
323 sediment fluxes set by the delta environment. Because bypassing does not appear to affect the
324 updrift shoreline orientation, we can write $Q_{s,u} = Q_{s,regional} - \frac{1}{2}Q_r$. The channel will migrate
325 downdrift if $Q_{s,u} > 0$, or, substituting into (2), if the *Sediment Source Ratio* $S > \frac{1}{2}$ assuming no
326 bypassing ($\beta = 0$) (Fig. 6). When some bypassing occurs ($\beta > 0$), the transition and degree of
327 downdrift migration is controlled by a combination of the *Sediment Source Ratio* S and the
328 bypassing fraction β (Fig. 6). Recognizing that the volume of updrift sediment blocked by the
329 river mouth scales with the relative alongshore sediment flux (S) that cannot bypass the channel

330 $(1-\beta)$, the ability of the deltaic channel to migrate downdrift can be described by the *Downdrift*
331 *Migration Index D*:

$$D = (1 - \beta) \cdot S. \quad (3)$$

332 For $D = 0$, there is either a symmetric wave climate ($Q_{s,regional} = 0$) or $\beta=1$, and the channel will
333 not migrate downdrift. D demonstrates that, as expected, some of the alongshore sediment
334 transport needs to be blocked by the river mouth to cause downdrift migration (see also Fig. 6).
335 For increasing values of D , the channel should be increasingly oriented downdrift away from the
336 direction of wave approach.

337 4.4.3 *Updrift migration*

338 Similarly, we can investigate what flux combinations lead to updrift migration. For small
339 cusped deltas that do not significantly reorient their shorelines, the channel does not migrate
340 because the shoreline orientation is symmetrical updrift and downdrift of the river mouth. This
341 symmetry is disturbed if, because of large fluvial sediment supply (high Q_r) or a very
342 asymmetric wave climate ($Q_{s,regional}$ approaching $Q_{s,d,max}$), the downdrift coastline would need to
343 transport more than what it can maximally accommodate through shoreline reorientation (i.e., if
344 $Q_{s,regional} + \frac{1}{2}Q_r > Q_{s,d,max}$). In this case, the additional fluvial sediment flux will have to be moved
345 away from the channel along the updrift coast, accommodated through reorientation of the
346 updrift flank's shoreline. Asymmetry in the shoreline angles around the river mouth associated
347 with this reorientation causes updrift migration of the channel, regardless of the direction of
348 sediment transport updrift of the channel ($Q_{s,u}$ positive or negative). However, in most of our

349 model simulations, the large fluvial sediment supply that caused reorientation of the updrift delta
350 flank resulted in reversal in the direction of updrift sediment transport (Fig. 5e).

351 Cast into alongshore sediment transport fluxes, the channel will migrate updrift when the
352 alongshore sediment transport that would need to be conveyed by the downdrift flank ($\frac{1}{2}Q_r +$
353 $\beta \cdot Q_{s,regional}$) in a symmetrical configuration is larger than the maximum potential sediment
354 transport ($Q_{s,d,max}$):

$$\frac{1}{2}Q_r + \beta \cdot Q_{s,regional} > Q_{s,d,max}, \quad (4)$$

355 or, rearranging using $Q_{s,d,max} = \frac{1}{2} Q_{s,max}$,

$$1 + 2\beta \cdot \frac{Q_{s,regional}}{Q_r} > \frac{Q_{s,max}}{Q_r}, \quad (5)$$

356 and rewriting in terms of the *River Dominance Ratio* R and the *Sediment Source Ratio* S , we
357 define the *Updrift Migration Index* U :

$$U = R(1 + 2 \cdot \beta S). \quad (6)$$

358 where channels migrate updrift if $U > 1$. For $U < 1$, fluvial sediment supply is insufficient to
359 force updrift migration, and the channel will either be symmetric or migrate downdrift. If no
360 alongshore sediment is able to bypass ($\beta = 0$), the channel should switch from downdrift to
361 updrift migration when $R = 1$. If alongshore sediment can bypass the mouth ($\beta > 0$), updrift
362 migration can occur for lower fluvial sediment supply rates, as bypassed sediment from the
363 updrift coastline brings the downdrift flank closer to $Q_{s,d,max}$.

364 Note that even though the transition from downdrift to updrift migration is dependent on
365 alongshore sediment bypassing, the channel orientation of an updrift-migrating channel becomes
366 less dependent on bypassing for increasing fluvial sediment supply. For high fluvial sediment
367 supply $S \ll R$, such that $U \approx R$ (eq. 6) and U then becomes independent of β . This is intuitive
368 because for high fluvial sediment supply, net littoral transport along the updrift flank is directed
369 away from the river mouth ($Q_{s,l} < 0$) such that littoral sediment is rarely transported across the
370 river mouth and therefore bypassing is unimportant

371 4.4.5 Updrift and downdrift migration in model results

372 Investigating channel orientation across a wide variety of fluvial sediment supply
373 conditions, wave heights, angular distributions of incoming wave energy, and alongshore
374 sediment bypassing fractions, we find that the *Updrift Migration Index* U (eq. 6) and the
375 *Downdrift Migration Index* D (eq. 3) effectively explain the variety in modeled channel
376 orientations (Fig. 7a). Channel orientations in the space defined by U and D vary smoothly;
377 channels migrate downdrift for large values of D and updrift for large U . Updrift channel
378 orientations increase for more asymmetric wave climates. This occurs in part because if the wave
379 climate is symmetrical ($S = 0$), there is no “updrift” or “downdrift”, and the channel will not
380 migrate even if $U > 1$.

381 4.5 Comparison to natural examples

382 We use our model simulations to derive a predictive framework of channel orientation,
383 fitting a smooth contour mapping onto our model-derived results to link U and D to a channel
384 orientation (Fig. 7b). R and S (and therefore U and D for an assumed alongshore sediment

385 bypassing fraction) can be determined *a priori*, allowing us to test this channel orientation
386 framework for natural deltas. We calculate R and S for 10 natural deltas (or delta lobes) using
387 NOAA WaveWatch III data (Chawla et al., 2013) and published fluvial sediment fluxes (see
388 Supplemental Table 1). We measured the regional shoreline orientation by connecting the updrift
389 and downdrift coast at the locations closest to the river mouth where their orientations align.

390 Unfortunately, long-term bypassing rates are unknown for most natural case samples,
391 partially because direct measurements of such rates are difficult to measure. This limitation does
392 not apply to deltas with nearly (but not completely) symmetric wave climates ($S \rightarrow 0$ but $S > 0$)
393 with large U (Rosetta, Nile) where the channel orientation is mostly independent of the
394 bypassing fraction (Fig. 7b).

395 However, for asymmetric wave climates and an unknown bypassing fraction, there is
396 only a limited space within Fig 7B that the delta can plot (shown by the dashed lines for the
397 Danube and the Sao Francisco), such that our predictive framework can be used to determine if a
398 delta's channel orientation suggests significant bypassing. Starting with an initial assumption of
399 no bypassing ($\beta = 0$), the tendency for deltaic channels to either grow into (blue shades) or away
400 from (red shades) the dominant wave direction coincides with the predictive framework for all
401 cases except for the Danube and the Sao Francisco (Fig. 7b). This provides a general prediction
402 that bypassing is low for most of the cases with large S . The general agreement between our
403 prediction and the test cases suggests that wave climate asymmetry and fluvial sediment supply
404 are primary controls on channel orientation for these deltas, and that the modeled dynamics in

405 our exploratory coastline model are appropriate for the representation of large-scale delta
406 morphology.

407 Assuming $\beta = 0$ overestimated the downdrift orientation of the channels for the St.
408 George lobe of the Danube and the Sao Francisco, suggesting that bypassing is likely significant
409 for these deltas. For these two cases, we can apply our predictive framework to infer the fraction
410 of alongshore sediment bypassing. In the space defined by U and D , the bypassing fraction β
411 follows a linear trajectory from $U = R$ and $D = S$ (for $\beta = 0$) to $U = R(1+2S)$ and $D = 0$ (for $\beta =$
412 1). We can follow the trajectory for increasing bypassing to match an observed channel
413 orientation with an unknown bypassing fraction (dashed lines in Fig. 7b).

414 The St. George lobe of the Danube delta shows a symmetrically growing channel (Fig.
415 1d). For $\beta = 0$, the framework predicts a downdrift deflection of about 10° . Following the
416 trajectory for increasing β (dashed line in Fig. 7b), we find that an efficient bypassing regime (β
417 approaching 1) compares best to the observed channel orientation. Although quantitative
418 measurements have yet to be performed for alongshore sediment bypassing around the Danube,
419 the possibility of an efficient bypassing regime has been suggested by Giosan (2007) based upon
420 the existence of a large subaqueous platform in front of the river mouth promoting wave
421 breaking and alongshore sediment bypassing.

422 The Sao Francisco River delta channel is also reoriented downdrift to a smaller extent
423 (15°) than what the $\beta = 0$ scenario would predict (35° , Fig. 7b). Using our predictive framework,
424 we find our model simulations at $U = \frac{2}{3}$ and $D = \frac{1}{10}$ generate channel orientations of 15° (Fig.

425 7b). For the Sao Francisco, with a *Sediment Source Ratio* $S = 1$, and the *River Dominance Ratio*
426 $R = 0.3$ (Supplemental Table 1, Dominguez, 1996), this leads to a predicted long-term bypassing
427 fraction of $\beta = 0.6$.

428 Using predicted bypassing fractions, we can also estimate the relative proportion of
429 coarse-grained sediment from the updrift littoral system versus fluvially sourced sediment in the
430 downdrift delta flank. For the Sao Francisco, with $\beta = 0.6$ and $S = 1$, and using $Q_{s,u} = Q_{s,regional} -$
431 $\frac{1}{2}Q_r$, we estimate that $\beta Q_{s,u} = \frac{6}{10}(Q_{s,regional} - \frac{1}{2}Q_r) = \frac{3}{10}Q_r$ of the downdrift flux is littoral
432 material sourced from the updrift flank. Compared to 1 Q_r that is sourced from the river, we
433 estimate that $\frac{10}{13}$ of the downdrift coarse-grained flux should be fluvially derived. This
434 dominance of fluvially derived sediment on the downdrift flank qualitatively agrees with
435 analyses of the Sao Francisco beach median grain size that indicate that the downdrift flank is
436 composed of less mature (fluvially derived) sands of about 0.23 mm whereas the updrift flank is
437 composed of 0.125 mm sands (Barbosa and Dominguez, 2004).

438 4.6 *Change in sediment supply*

439 Our modeling results suggest that deltas experiencing changes in wave climate or fluvial
440 sediment supply should see a corresponding shift in their channel orientation at the coastline.
441 Such changes have also been observed on natural deltas. For example, noting the channel
442 orientation of the Arno and Ombrone deltas in Italy, Pranzini (2001) suggested that a change
443 from downdrift to updrift migration occurred as a response to land-use changes that increased the
444 fluvial sediment flux.

445 To investigate the response of the channel orientation of a wave-influenced delta to
446 changes in the fluvial sediment supply, we ran a modeling scenario resembling the case of the
447 Ombrone delta. In this simulation, we first grow a delta with a low fluvial sediment supply and
448 no alongshore sediment bypassing ($\beta = 0$) such that a downdrift migrating channel develops.
449 Then, we increase the fluvial sediment supply under a constant wave climate. We find that for an
450 increase in sediment supply, the channel orientation rapidly adjusts from downdrift to updrift
451 migration (Fig. 8). The steady-state channel orientations for both the low flux and high flux
452 periods agree with the predictive framework (markers on Fig. 7b).

453 To investigate if a fluvial sediment supply decrease has a similar effect on channel
454 orientation, we extend the previously described scenario and now decrease fluvial sediment
455 supply back to 40 kgs^{-1} (Fig. 8b). Interestingly, because the decrease initiated partial
456 abandonment and retreat of the river mouth, we find a significant delay before the channel again
457 attains its original orientation (Fig. 8c). Even though the channel still supplies fluvial sediment to
458 the coast, the river mouth temporarily erodes and ceases to prograde for an extended period.
459 Focused erosion around the river mouth occurs because the flanks of the delta are oriented to
460 transport more littoral sediment to the distal flanks than they now receive from the river mouth.
461 This negative (local) sediment budget results in a pulse of coastline retreat diffusing outwards
462 away from the river mouth even as the distal portions of the delta continue to grow, with
463 potentially important consequences not only for interpretations of modern deltaic change but also
464 the stratigraphic record of delta growth (Madof et al., 2016).

465 **5 Discussion**

466 *5.1 Implications for delta predictions and paleo-environmental reconstructions*

467 Model explorations performed here show how deltaic channel orientation can respond to
468 long-term environmental conditions via feedbacks with wave-driven alongshore sediment
469 transport (Fig. 5). For known directional wave climate, fluvial sediment supply, and alongshore
470 sediment bypassing we can calculate U and D (eq. 3 and 6), which determine the resulting
471 steady-state channel orientation in accordance with our model simulations and natural examples
472 (Fig. 7b).

473 Following the same approach, our framework (Fig. 7b) also offers new possibilities for
474 paleo-environmental reconstructions. From an observed channel orientation and an alongshore
475 sediment bypassing fraction (inferred for instance from the channel size, see Nienhuis et al.,
476 2016), we can determine both the *River Dominance Ratio* R and the *Sediment Source Ratio* S . R
477 offers insight into the gross morphology of the river delta (Nienhuis et al., 2015), and S can be
478 used to characterize the delta's sedimentological asymmetry (Dominguez, 1996; Giosan, 1998).
479 Additionally, the product of R and S (equal to $Q_{s,regional}/Q_{s,max}$), which can be determined from
480 just the channel orientation, provides a novel measure of wave climate directionality. For $R:S = 0$,
481 where the framework suggests a delta channel perpendicular to the regional coastline, the wave
482 climate is predicted to be fully symmetrical (equal contributions of wave energy from the left
483 and right regional coastline). At the other extreme, if $R:S = 1/2$ ($Q_{s,regional} = 1/2 Q_{s,max} = Q_{s,r,max}$), the
484 wave climate is fully asymmetrical. Note that this is not a measure of local wave climate
485 asymmetry at a single alongshore location, but rather of the deep-water wave climate, referenced
486 from the regional coastline and independent of delta dynamics. Examples of natural systems that

487 lend themselves to such a reconstruction are the Arno and the Ombrone deltas in Italy (Pranzini,
488 2001), the Jequitinhonha, the Sao Francisco, and the Doce deltas in Brazil (Rossetti et al., 2015),
489 and the Cretaceous San Miguel Formation (Bhattacharya and Giosan, 2003).

490 5.2 *Effect of fluvial water discharge*

491 Our model explorations of wave-influenced deltas suggest that, in all cases, the channel
492 orientation of wave-influenced deltas should generally become increasingly updrift for
493 increasing fluvial sediment supply (Fig. 4). High fluvial water discharge, on the other hand, is
494 associated with low alongshore sediment bypassing (Kirk, 1991; Nienhuis et al., 2016), which
495 for low fluvial sediment supply should result in downdrift migrating channels. Combined, the
496 influence of fluvial sediment supply and fluvial discharge on channel orientations suggest that
497 fluvial sediment concentration (fluvial coarse-grained sediment supply divided by discharge)
498 may play an important role in controlling delta morphology. Deltas fed by a channel with low
499 fluvial sediment concentration should tend to migrate downdrift, as the relatively high discharge
500 will limit bypassing. In contrast, deltas fed with a high fluvial sediment concentration, with a
501 relatively large fluvial sediment supply, should tend to migrate updrift.

502 5.3 *Channel orientation for low fluvial sediment supply*

503 For low fluvial sediment flux or high wave energy, river mouths are not able to reorient
504 the coastline (Nienhuis et al., 2015). These small channels, however, are often ‘deflected’
505 (Bhattacharya and Giosan, 2003) and show downdrift migration along an otherwise straight
506 coastline. River mouth processes likely dictate at this scale, such that the dynamics that set
507 channel orientation are not determined by fluvial sediment supply, but rather by alongshore

508 sediment bypassing (Kirk, 1991; Nienhuis et al., 2016). When downdrift migration occurs
509 without the net progradation typical of river deltas, channel orientation is generally variable, as
510 spit breaching will reset the channel orientation on decadal timescales (Zenkovich, 1967).
511 Because our model sets the channel direction by the local shoreline orientation, downdrift
512 migration in our study requires coastline reorientation. The smallest-scale downdrift migrating
513 channel our model can resolve therefore must extend on the order of a few river mouth widths
514 offshore (e.g., Fig. 1c).

515 5.4 *Coarse-grained assumption*

516 We assume that fluvially derived fine-grained sediment does not significantly contribute
517 to the processes controlling subaerial plan-view delta shape. Even though this is generally a
518 reasonable assumption for deltas primarily shaped by alongshore sediment transport (Limber et
519 al., 2008), river mouths on asymmetric deltas can act as traps of fine-grained material on the
520 downdrift flank, resulting in series of shoreface sands separated by finer grained deposits
521 (Bhattacharya and Giosan, 2003). Further research is needed to investigate how much fine-
522 grained sediment contributes to the overall mass balance (and shoreline orientations) of wave-
523 influenced deltas.

524 5.5 *Shoreline-parallel bathymetry contours*

525 CEM assumes that waves refract across shoreline-parallel contours and that alongshore
526 sediment flux divergence is linearly related to shoreline change (Ashton and Murray, 2006a).
527 With this assumption, the model collapses vertical delta dynamics down to a single contour line.
528 A drawback is that the parallel contour line assumption neglects the sometimes complex

529 bathymetry that characterizes many wave-influenced deltas. In particular, deltas that develop in
530 an asymmetric wave climate often show large subaqueous platforms downdrift that reduce the
531 local downdrift wave energy (Correggiari et al., 2005; Giosan, 2007; Giosan et al., 2005), and
532 therefore violate the one-contour-line assumption (Falqués and Calvete, 2005). However, as our
533 analysis suggests that the channel orientation is controlled by the updrift flank sediment flux
534 partitioning, delta mouth dynamics may be relatively independent of the downdrift delta flank
535 unless there is significant coastline reorientation.

536 **6 Conclusion**

537 In this study we have investigated how feedbacks between the directional wave climate,
538 fluvial sediment supply, and alongshore sediment bypassing can determine the channel
539 orientation of wave-influenced deltas. Modeling results enabled us to formulate key criteria for
540 updrift and downdrift channel migration. In particular, we found that limiting alongshore
541 sediment bypassing of river mouths should tend to drive downdrift channel migration. On the
542 other hand, deltaic channels are expected to migrate updrift when the magnitude of the fluvial
543 sediment supply causes the downdrift flank to reach the angle of maximum alongshore transport,
544 a phenomenon that can occur both with and without alongshore sediment bypassing. Translating
545 modeling results into a predictive framework shows good agreement with natural examples,
546 providing an approach to estimate the long-term alongshore sediment bypassing of river mouths.
547 Additionally, we find that the deltaic channel orientation can respond dynamically to fluvial
548 sediment supply changes, highlighting the potential of plan-view delta geometry to backtrack
549 climate and land-use changes.

550 **7 Acknowledgements**

551 This study was supported by NSF grant EAR-0952146. We acknowledge helpful reviews
552 by an anonymous reviewer and the editor An Yin.

553 **8 References**

- 554 Aibulatov, N.A., Shadrin, I.F., 1961. Some data on the long-shore drift of sand near natural
555 obstacles. Tr. Inst. Okeanol. Akad. Nauk. SSSR 53.
- 556 Ashton, A.D., Giosan, L., 2011. Wave-angle control of delta evolution. Geophys. Res. Lett. 38,
557 L13405. doi:10.1029/2011GL047630
- 558 Ashton, A.D., Hutton, E.W.H.H., Kettner, A.J., Xing, F., Kallumadikal, J., Nienhuis, J.H.,
559 Giosan, L., 2013. Progress in coupling models of coastline and fluvial dynamics. Comput.
560 Geosci. 53, 21–29. doi:10.1016/j.cageo.2012.04.004
- 561 Ashton, A.D., Murray, A.B., 2006a. High-angle wave instability and emergent shoreline shapes:
562 1. Modeling of sand waves, flying spits, and capes. J. Geophys. Res. 111, F04011.
563 doi:10.1029/2005JF000422
- 564 Ashton, A.D., Murray, A.B., 2006b. High-angle wave instability and emergent shoreline shapes:
565 2. Wave climate analysis and comparisons to nature. J. Geophys. Res. 111, F04012.
566 doi:10.1029/2005JF000423
- 567 Ashton, A.D., Murray, A.B., Arnoult, O., 2001. Formation of coastline features by large-scale
568 instabilities induced by high-angle waves. Nature 414, 296–300. doi:10.1038/35104541
- 569 Bakker, W.T.J.N.P., Edelman, T., 1964. The Coastline of River-deltas, in: Edge, B. (Ed.), Proc.
570 of the 9th Conf. on Coastal Engineering. ASCE, Lisbon, pp. 199–218.
571 doi:10.9753/icce.v9.%25p
- 572 Balouin, Y., Ciavola, P., Michel, D., 2006. Support of Subtidal Tracer Studies to Quantify the
573 Complex Morphodynamics of a River Outlet: the Bevano, NE Italy. J. Coast. Res. 1, 602–
574 606.
- 575 Barbosa, L.M., Dominguez, J.M.L., 2004. Coastal dune fields at the São Francisco River
576 strandplain, northeastern Brazil: morphology and environmental controls. Earth Surf.
577 Process. Landforms 29, 443–456. doi:10.1002/esp.1040
- 578 Bates, C.C., 1953. Rational theory of delta formation. Am. Assoc. Pet. Geol. Bull. 37, 2119–
579 2162.
- 580 Bhattacharya, J.P., Giosan, L., 2003. Wave-influenced deltas: geomorphological implications for
581 facies reconstruction. Sedimentology 50, 187–210. doi:10.1046/j.1365-3091.2003.00545.x
- 582 Chawla, A., Spindler, D.M., Tolman, H.L., 2013. Validation of a thirty year wave hindcast using

- 583 the Climate Forecast System Reanalysis winds. *Ocean Model.* 70, 189–206.
584 doi:10.1016/j.ocemod.2012.07.005
- 585 Cooper, J.A.G., 1994. Sedimentary processes in the river-dominated Mvoti estuary, South
586 Africa. *Geomorphology* 9, 271–300. doi:10.1016/0169-555X(94)90050-7
- 587 Correggiari, A., Cattaneo, A., Trincardi, F., 2005. The modern Po Delta system: Lobe switching
588 and asymmetric prodelta growth. *Mar. Geol.* 222, 49–74. doi:10.1016/j.margeo.2005.06.039
- 589 Dominguez, J.M.L., 1996. The Sao Francisco strandplain: a paradigm for wave-dominated
590 deltas? *Geol. Soc. London, Spec. Publ.* 117, 217–231. doi:10.1144/GSL.SP.1996.117.01.13
- 591 Falqués, A., Calvete, D., 2005. Large-scale dynamics of sandy coastlines: Diffusivity and
592 instability. *J. Geophys. Res.* 110, C03007. doi:10.1029/2004JC002587
- 593 Geleynse, N., Storms, J.E.A., Walstra, D.-J.R., Jagers, H.R.A., Wang, Z.B., Stive, M.J.F., 2011.
594 Controls on river delta formation; insights from numerical modelling. *Earth Planet. Sci.*
595 *Lett.* 302, 217–226. doi:10.1016/j.epsl.2010.12.013
- 596 Giosan, L., 2007. Morphodynamic Feedbacks on Deltaic Coasts: Lessons from the Wave-
597 Dominated Danube Delta. *Coast. Sediments '07.* doi:10.1061/40926(239)63
- 598 Giosan, L., 1998. Long term sediment dynamics of Danube delta coast, in: Dronkers, J.,
599 Scheffers, M. (Eds.), *Physics of Estuaries and Coastal Seas.* Balkema, Rotterdam, pp. 365–
600 376.
- 601 Giosan, L., Constantinescu, S., Filip, F., Deng, B., 2013. Maintenance of large deltas through
602 channelization: Nature vs. humans in the Danube delta. *Anthropocene* 1, 35–45.
603 doi:10.1016/j.ancene.2013.09.001
- 604 Giosan, L., Donnelly, J.P., Vespremeanu, E., Bhattacharya, J.P., Olariu, C., Buonaiuto, F.S.,
605 2005. River delta morphodynamics: examples from the Danube delta, *River Deltas:*
606 *Concepts, Models and Examples.* SEPM (Society for Sedimentary Geology).
607 doi:10.2110/pec.05.83
- 608 Grijm, W., 1960. Theoretical forms of shorelines, in: Edge, B. (Ed.), *7th Conference on Coastal*
609 *Engineering.* ASCE, Lisbon, pp. 197–202. doi:10.9753/icce.v7.11
- 610 Gulliver, F.P., 1896. Cuspate forelands. *Bull. Geol. Soc. Am.* 7, 399–422.
- 611 Hudson, P.F., Kesel, R.H., 2000. Channel migration and meander-bend curvature in the lower
612 Mississippi River prior to major human modification. *Geology* 28, 531. doi:10.1130/0091-
613 7613(2000)28<531:CMAMCI>2.0.CO;2
- 614 Jerolmack, D.J., Mohrig, D., 2007. Conditions for branching in depositional rivers. *Geology* 35,
615 463. doi:10.1130/G23308A.1
- 616 Kirk, R.M., 1991. River-beach interaction on mixed sand and gravel coasts: a geomorphic model
617 for water resource planning. *Appl. Geogr.* 11, 267–287. doi:10.1016/0143-6228(91)90018-5
- 618 Kolb, C.R., 1963. *Sediments Forming the Bed and Banks of the Lower Mississippi River and*

619 their Effect on River Migration. *Sedimentology* 2, 227–234. doi:10.1111/j.1365-
620 3091.1963.tb01216.x

621 Komar, P.D., 1973. Computer models of delta growth due to sediment input from rivers and
622 longshore transport. *Bull. Geol. Soc. Am.* 84, 2217–2226. doi:10.1130/0016-
623 7606(1973)84<2217:CMODGD>2.0.CO;2

624 Komar, P.D., 1971. Mechanics of Sand Transport on Beaches. *J. Geophys. Res.* 76, 713–721.
625 doi:10.1029/Jc076i003p00713

626 Lamb, M.P., Nittrouer, J. a., Mohrig, D., Shaw, J., 2012. Backwater and river plume controls on
627 scour upstream of river mouths: Implications for fluvio-deltaic morphodynamics. *J.*
628 *Geophys. Res. Earth Surf.* 117, 1–15. doi:10.1029/2011JF002079

629 Larson, M., Hanson, H., Kraus, N.C., 1987. Analytical solutions of the one-line model of
630 shoreline change. US Army Waterw. Exp. Stn., Vicksburg.

631 Limber, P.W., Patsch, K.B., Griggs, G.B., 2008. Coastal Sediment Budgets and the Littoral
632 Cutoff Diameter: A Grain Size Threshold for Quantifying Active Sediment Inputs. *J. Coast.*
633 *Res.* 2, 122–133. doi:10.2112/06-0675.1

634 Madof, A.S., Harris, A.D., Connell, S.D., 2016. Nearshore along-strike variability: Is the concept
635 of the systems tract unhinged? *Geology* 44, 315–318. doi:10.1130/G37613.1

636 Murray, A.B., 2003. Contrasting the goals, strategies and predictions associated with simplified
637 numerical models and detailed simulations, in: Wilcock, P.R., Iverson, R.M. (Eds.),
638 Prediction in Geomorphology. American Geophysical Union, Washington DC, USA, pp.
639 151–165. doi:10.1029/135GM11

640 Nienhuis, J.H., Ashton, A.D., Giosan, L., 2015. What makes a delta wave-dominated? *Geology*
641 43, 511–514. doi:10.1130/G36518.1

642 Nienhuis, J.H., Ashton, A.D., Nardin, W., Fagherazzi, S., Giosan, L., 2016. Alongshore sediment
643 bypassing as a control on river mouth morphodynamics. *J. Geophys. Res. Earth Surf.* 121.
644 doi:10.1002/2015JF003780

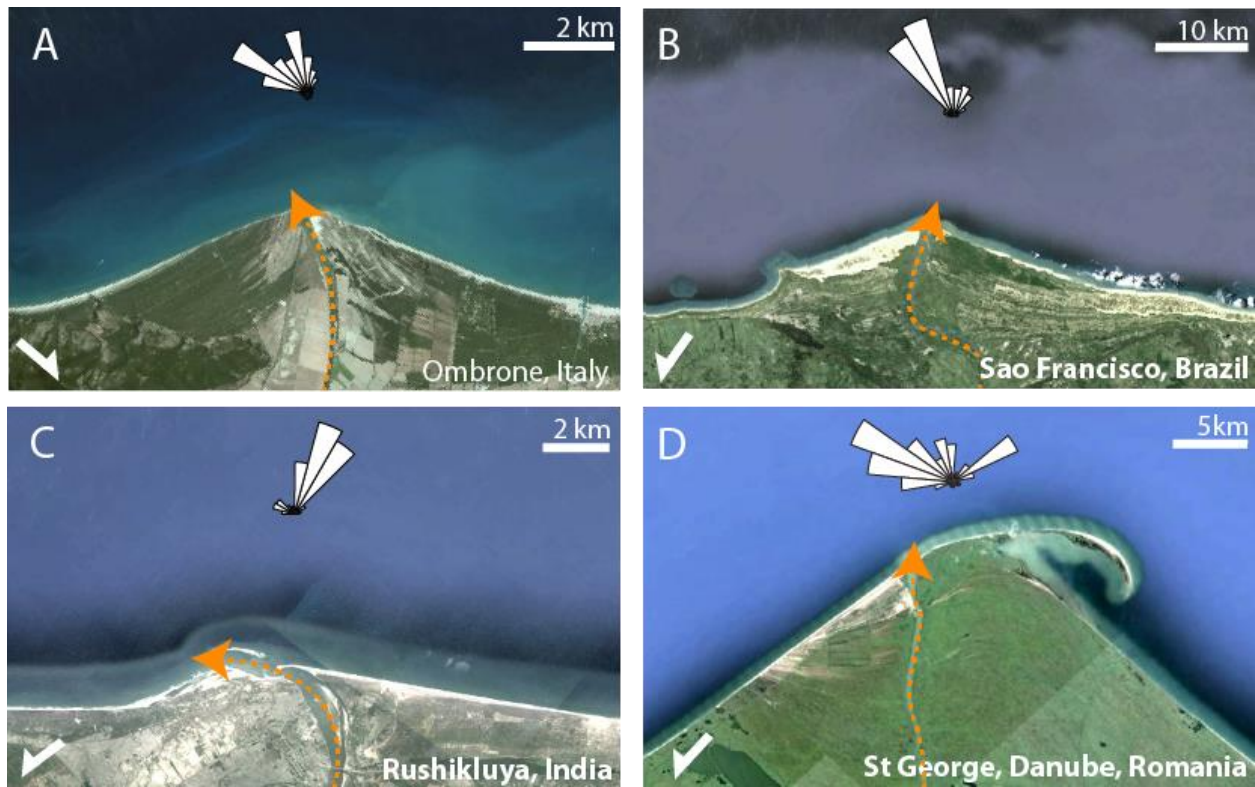
645 Nienhuis, J.H., Ashton, A.D., Roos, P.C., Hulscher, S.J.M.H., Giosan, L., 2013. Wave reworking
646 of abandoned deltas. *Geophys. Res. Lett.* 40, 5899–5903. doi:10.1002/2013GL058231

647 Pranzini, E., 2001. Updrift river mouth migration on cusped deltas: two examples from the coast
648 of Tuscany (Italy). *Geomorphology* 38, 125–132. doi:10.1016/S0169-555x(00)00076-3

649 Roelvink, J.A., Boutmy, A., Stam, J., 1998. A simple method to predict long-term morphological
650 changes, in: Edge, B.L. (Ed.), Coastal Engineering 1998. ASCE, Copenhagen, Denmark,
651 pp. 3224–3237.

652 Rossetti, D. de F., Polizel, S.P., Cohen, M.C.L., Pessenda, L.C.R., 2015. Late Pleistocene–
653 Holocene evolution of the Doce River delta, southeastern Brazil: Implications for the
654 understanding of wave-influenced deltas. *Mar. Geol.* 367, 171–190.
655 doi:10.1016/j.margeo.2015.05.012

- 656 Tanner, W.F., 1958. The equilibrium beach. *Trans. Am. Geophys. Union* 39, 889.
657 doi:10.1029/TR039i005p00889
- 658 Wright, L.D., 1977. Sediment Transport and Deposition at River Mouths - Synthesis. *Geol. Soc.*
659 *Am. Bull.* 88, 857–868. doi:10.1130/0016-7606(1977)88<857
- 660 Wright, L.D., Coleman, J.M., 1973. Variations in morphology of major river deltas as functions
661 on ocean wave and river discharge regimes. *Am. Assoc. Pet. Geol. Bull.* 57, 370–398.
- 662 Zenkovich, V.P., 1967. *Processes of Coastal Development*, 1st ed. Oliver & Boyd, Edinburgh.



663

664

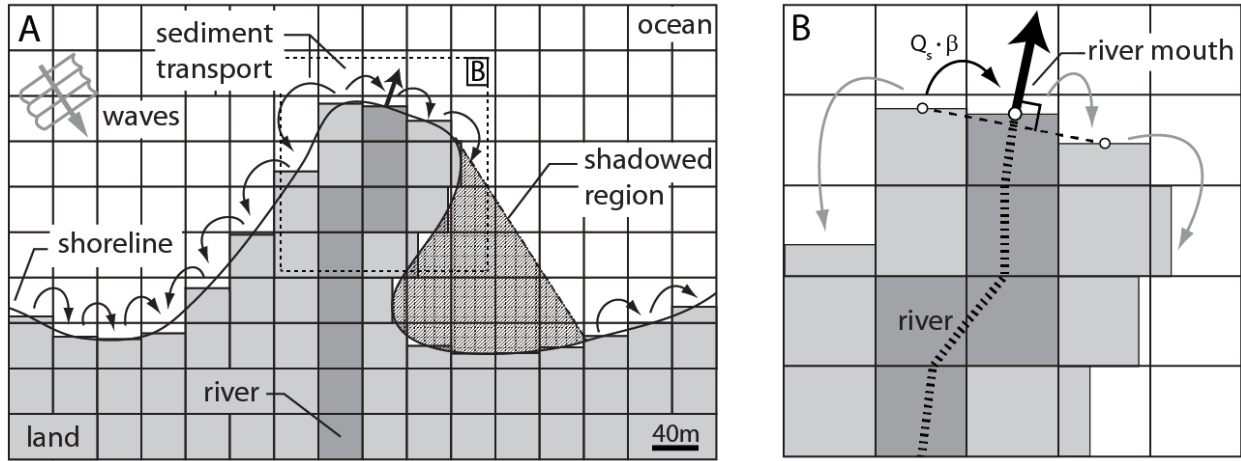
665

666

667

668

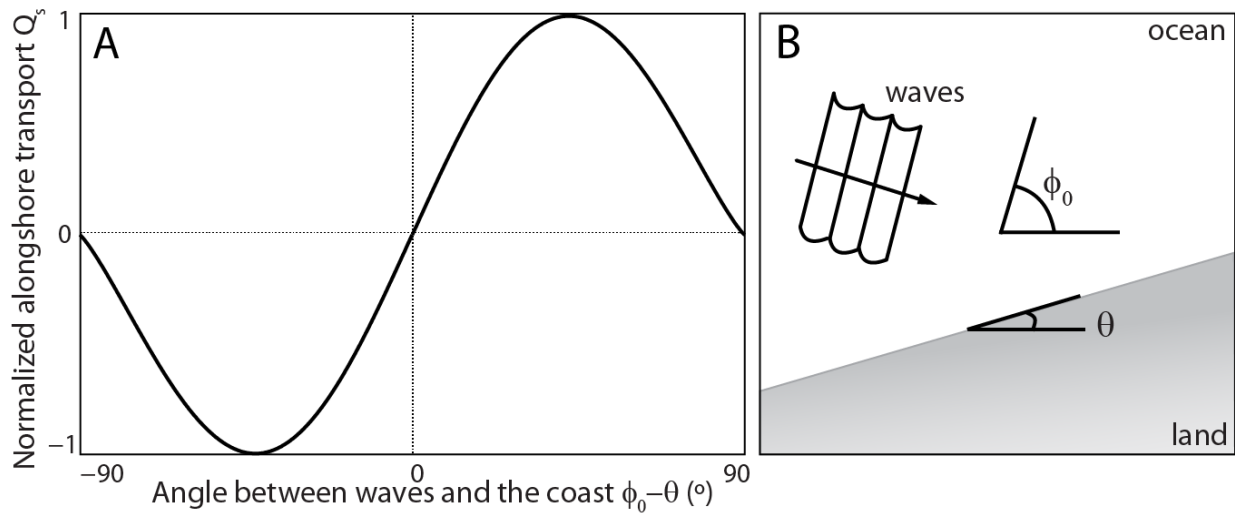
Figure 1. Examples of wave-influenced deltas with differing channel orientations in relation to the wave direction. (A) Ombrone, Italy, (B) Sao Francisco, Brazil, (C) Rushikulya, India and (D) Danube, Romania. The orange arrows indicate the active channels on these deltas. Wave roses show the angular distribution of wave energy, wave data from NOAA WaveWatch III® (Chawla et al., 2013). Images © Google Earth.



669

670 **Figure 2.** (A) Alongshore sediment flux Q_s as a function of the deep-water wave approach angle,
 671 normalized to $Q_{s,d,max}$. (B) Definition of the deep-water wave approach angle and the local
 672 shoreline orientation.

673



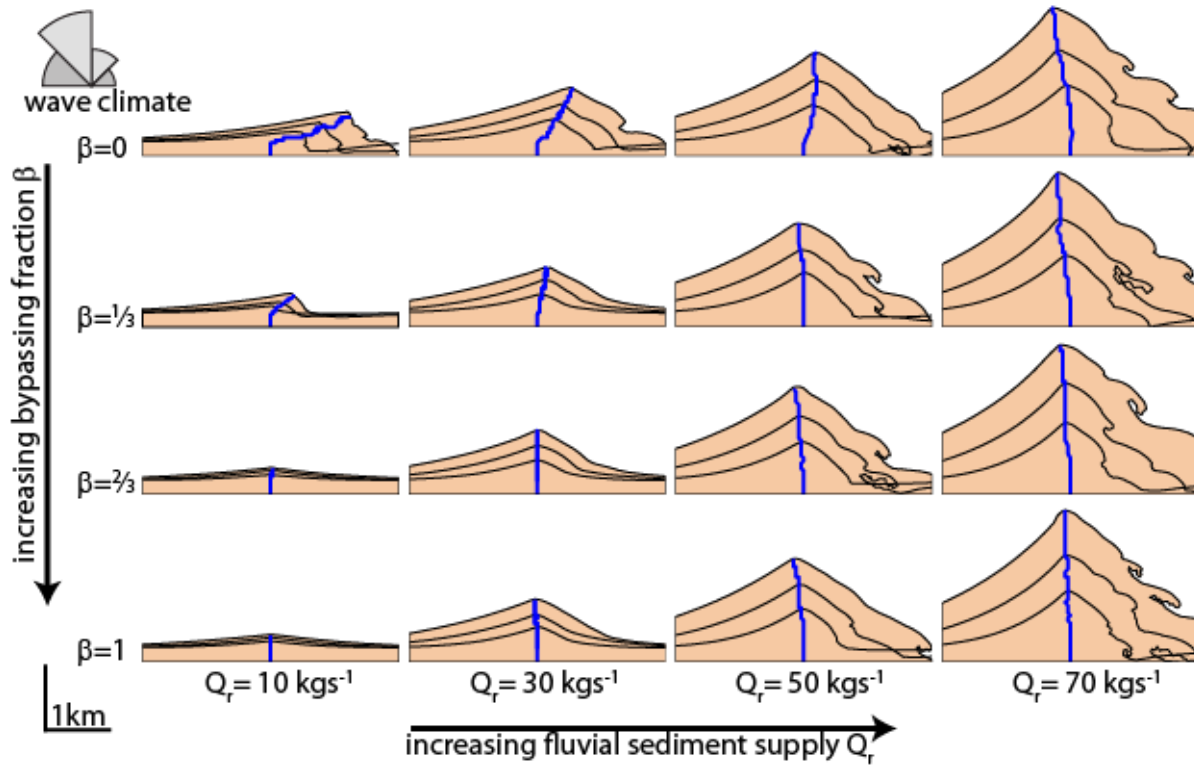
674

675 **Figure 3.** (A) Model domain schematic of CEM. The dashed box is enlarged in panel B. (B)

676 Schematic depiction of the two modifications to CEM: the ability of the channel to reorient itself

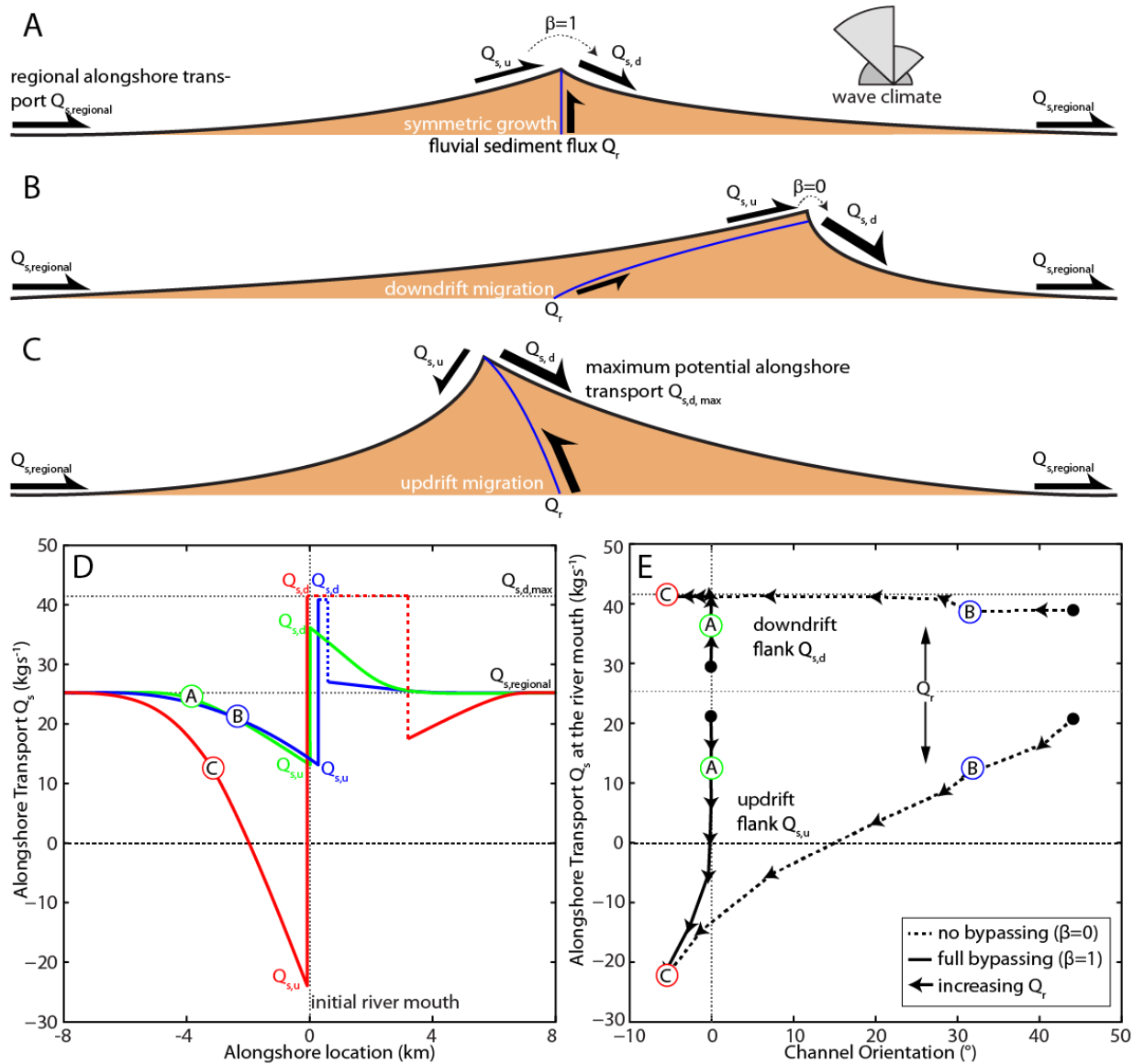
677 to be perpendicular to the local shoreline orientation and the restriction in alongshore sediment

678 flux allowed to bypass the river mouth cell by a fraction β .



679

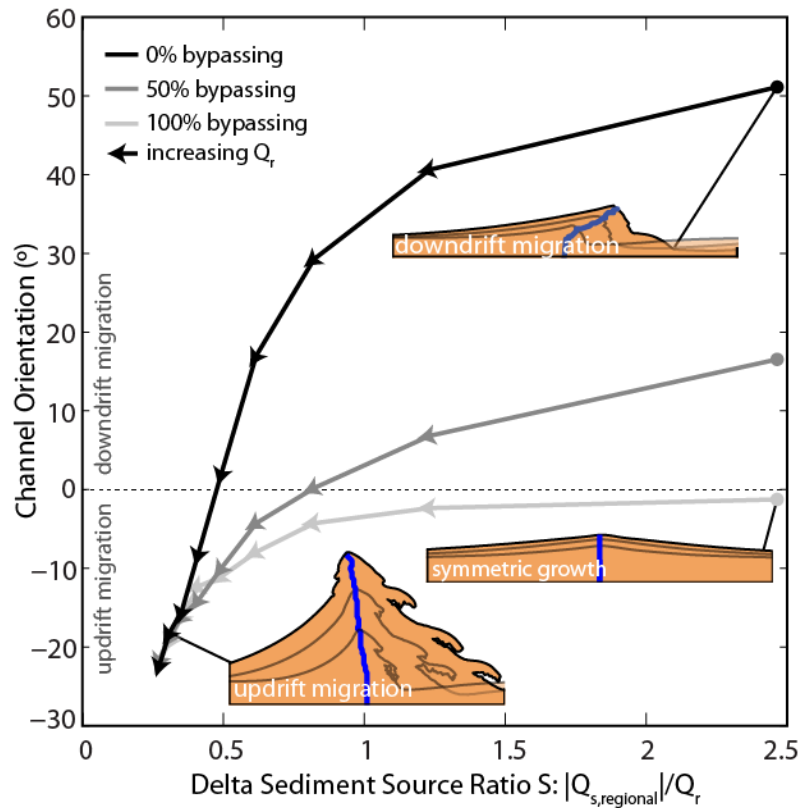
680 **Figure 4.** Examples of modeled wave-influenced deltas for different fluvial sediment supply
 681 rates and different bypassing fractions, β . The black lines indicate the shoreline position every 20
 682 model years. All results here have the same wave climate, with 1 m waves, $A = 0.8$, and $H = 0.3$,
 683 as represented by rose of the angular distribution of incoming wave energy.



684

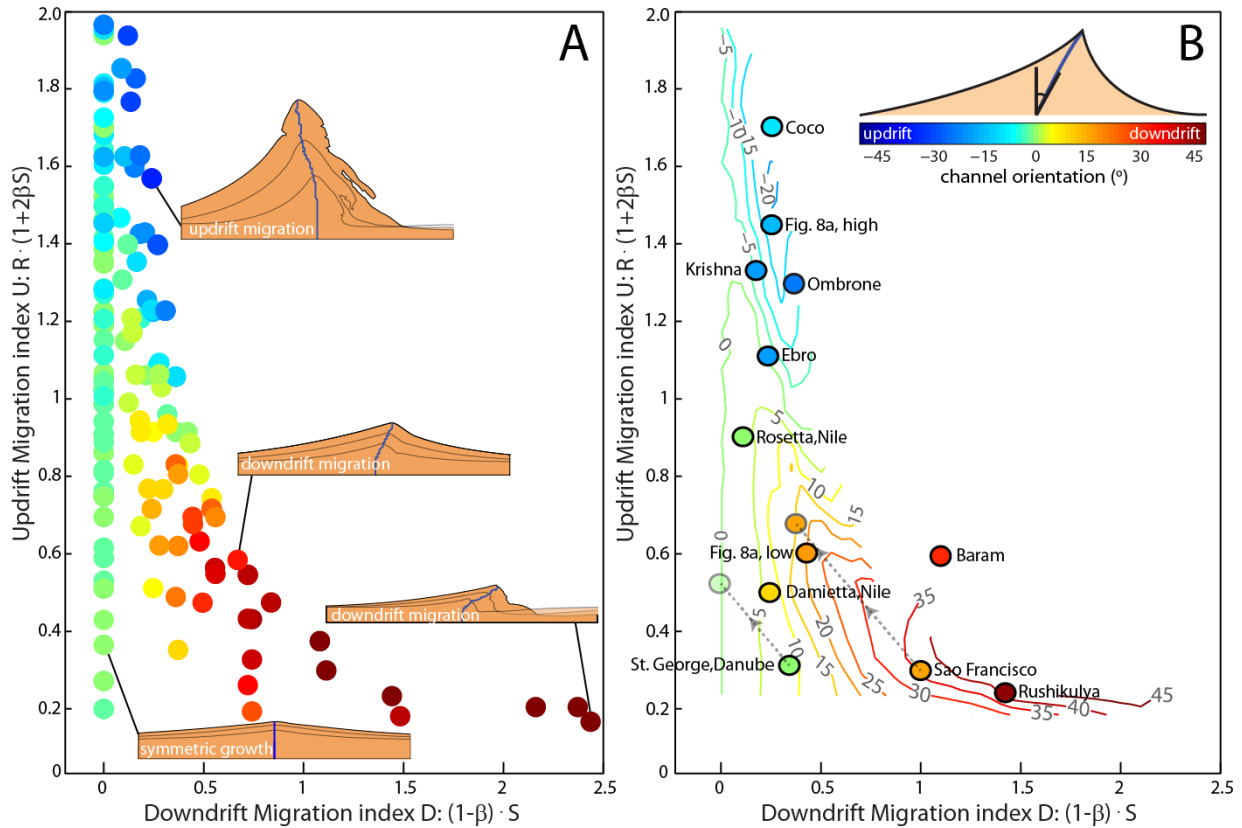
685 **Figure 5.** Flux definitions for three schematized model experiments showing (A) symmetric
 686 growth ($R = 0.3$, $S = 0.9$, $\beta = 1$), (B) downdrift migration ($R = 0.3$, $S = 0.9$, $\beta = 0$), and (C)
 687 updrift migration ($R = 1.1$, $S = 0.3$, $\beta = 0$). Arrows scale with the magnitude and direction of the
 688 littoral and fluvial sediment flux. The wave rose represents the area-weighted angular
 689 distribution of incoming wave energy. $A = 0.8$, $H = 0.1$. (D) Long-term average alongshore

690 sediment fluxes of three model runs schematized in panels A, B and C. Dashed portions of the
691 lines represent when the deltaic shoreline has reached $Q_{s,r,max}$. The increase in alongshore
692 sediment transport rate Q_s when moving across the river mouth equals the fluvial sediment flux
693 Q_r . (E) Average alongshore sediment fluxes to the left and right of the river mouth ($Q_{s,l}$ and $Q_{s,r}$,
694 the peaks in panel D) plotted against the channel orientation for modeled deltas with differing
695 fluvial sediment fluxes ranging from 10 kgs^{-1} to 80 kgs^{-1} , with arrows, plotted for different model
696 runs, pointing in the direction of increasing fluvial sediment flux.



698

699 **Figure 6.** Channel orientation for different values of the *Sediment Source Ratio* S for varying
700 bypassing rates and fluvial sediment supply Q_r (10 to 80 kgs^{-1}) for the same wave climate ($A =$
701 0.8, $H = 0.1$). Arrows point in the direction of increasing Q_r . Three model runs provide examples
702 of delta morphology for different channel orientations.



703

704

705

706

707

708

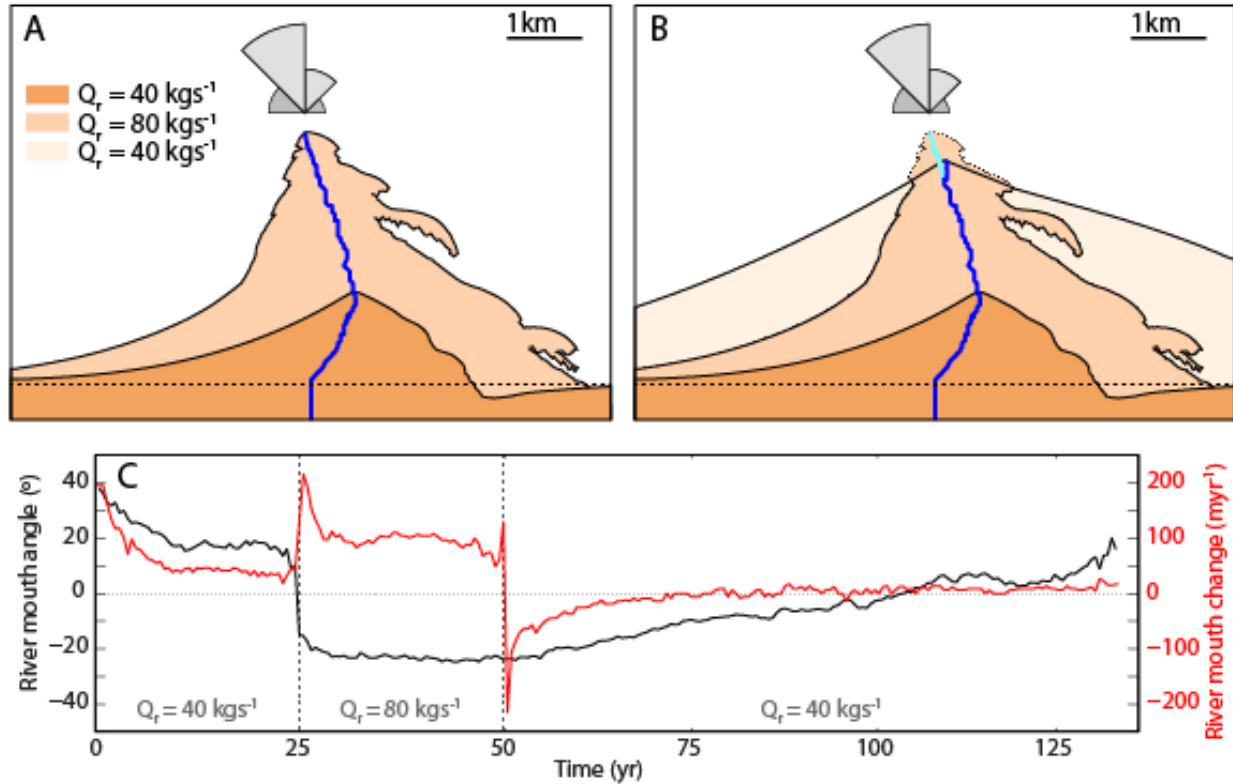
709

710

711

712

Figure 7. (A) Channel orientation of modeled deltas (color-coded, inset in panel B shows angle definition, positive in the direction of regional littoral drift.) for different values of D and U . Four model runs provide examples of delta morphology for different channel orientations. (B) Predictive framework of the channel orientation of wave-influenced deltas, plotted as contours of the channel orientation (in degrees) in the space defined by D and U . Markers are natural examples of wave-influenced deltas, plotted assuming $\beta = 0$. The dashed lines show the trajectory of the Sao Francisco and the Danube delta for increasing bypassing up to the inferred bypassing fraction. Two markers show the low and high flux channel orientation of the experiment of Fig. 8a.



713
 714 **Figure 8.** (A) Channel orientation response to an increase in fluvial sediment supply (40 kgs^{-1} to
 715 80 kgs^{-1}), changing the *Sediment Source Ratio* S from 0.6 to 0.3, and increasing the *River*
 716 *Dominance Ratio* R from 0.6 to 1.2. (B) Channel orientation response to a subsequent decrease in
 717 fluvial sediment supply (80 kgs^{-1} to 40 kgs^{-1}). Initially the river mouth retreats (light shaded blue
 718 channel) before progradation can set a new orientation (dark shaded blue channel). Inset shows
 719 distribution of incoming wave energy. Dotted lines indicate the initial coastline. (C) River mouth
 720 angle (black) and river mouth progradation rate (red) of the delta in panels A and B. Vertical
 721 dotted lines indicate time of fluvial sediment supply change.